IEEE Access
Multidisciplinary | Rapid Review | Open Access Journal

Received October 7, 2019, accepted October 29, 2019, date of publication November 5, 2019, date of current version November 14, 2019.

Digital Object Identifier 10.1109/ACCESS.2019.2951724

Optimal Detection and Ambiguity Function of Hybrid Distributed MIMO Radar

QILEI ZHANG, ZHEN DONG, AND DEXIN LI
College of Electronics Science, National University of Defense Technology (NUDT), Changsha 410073, China

Corresponding author: Qilei Zhang (zhangqilei@nudt.edu.cn)

This work was supported in part by the National Natural Science Foundation of China under Grant 61501477 and Grant 61601008, and in part by the China Postdoctoral Science Foundation under Grant 2017M620856.

ABSTRACT This paper proposes a notional radar concept, named hybrid distributed multi-input multi-output (MIMO) radar, which brings together the distributed MIMO radar concept and the phased-array (PA) radar one. In particular, the hybrid distributed MIMO radar is composed of K sub-arrays which are randomly distributed with wide separations. Each sub-array consists of Q all-digital colocated antenna elements with T/R modules separated by half-wavelength inter-element spacing. In the transmitting end, each sub-array operating as a PA radar, is driven by an independent waveform that is orthogonal with waveforms transmitted by other sub-arrays. In the receiving end, the reflected signals are received by all elements in the whole array and jointly processed. The hybrid distributed MIMO radar is a promising technique, due to its capability of providing spatial diversity gains and high resolutions. In this paper, as the first stage of studying the target detection and localization problem for hybrid distributed MIMO radar, we present its signal model, and then develop the optimal detection theory and ambiguity function. Finally, sufficient numerical examples are provided to verify the effectiveness of the proposed radar system.

INDEX TERMS Radar, multi-input multi-output (MIMO), phased-array (PA), hybrid distributed MIMO, optimal detection, ambiguity function (AF).

I. INTRODUCTION

As a new array radar paradigm, the multi-input multi-output (MIMO) radar has been focused by the radar community in the last two decades [1]–[5]. It uses multiple antennas to simultaneously transmit multiple probing signals that may be orthogonal or partially correlated with each other [4]–[7], while it also uses multiple antennas to receive the reflected signals. Generally speaking, MIMO radars can be categorized into two main types depending on the array configuration [2], [3]. One is the colocated MIMO radar, for which the spacing of the antenna elements is in the level of half-wavelength; and the other one is the distributed (or statistical) MIMO radar, for which the antenna elements are widely separated. The colocated MIMO radar mainly exploits the waveform diversity to achieve improved parameter identifiability and enhanced flexibility of transmit beampattern design [2]. While, for the second type of MIMO radar, the target's spatial diversity can be exploited by widely separated transmit/receiver antennas. Therefore the distributed MIMO radar can be applied to overcome the radar cross section (RCS) scintillation which is like the channel fading in the wireless communications [3]. Furthermore, the distributed MIMO radar can also be applied to provide high resolution target localization, improved direction finding and moving target detection [8]–[11]. However, these advantages do not come free of cost. More transmit/receive channels, usually, lead to more complicated system realizations. The generation of large number of orthogonal waveforms is quite difficult both in the theoretical design and engineering realization [5]–[7]. Moreover, for the distributed MIMO radar, time and phase synchronizations are also required [3]. Note that recent progresses on the distributed transmit beamforming in the communication community provide the possibility of solving the synchronization issue in the distributed MIMO radar [12]. The detailed discussion of these techniques is beyond the scope of this paper.

Another important array radar paradigm is the phased-array (PA) radar, which has been well developed and widely used in many fields [13]. In contrast, the PA radar usually

The associate editor coordinating the review of this manuscript and approving it for publication was Mohsen Khalily.

transmits a single waveform using multiple antennas, and thus can exploit coherent processing gain and flexible beamforming abilities. There have been many comparisons and debates between the PA radar and the MIMO radar [14], [15]. In this paper, we would rather try to exploit jointly the benefits of these two techniques than discuss which one will supplant the other one. In fact, several relevant attempts have been done [16]–[21].

In [16]–[19], the hybrid MIMO phased-array radar (HMPAR) concept was proposed. The array organization of HMPAR is two-level hierarchical. At the higher level there are M transmitting units. The phase centers of these transmitting units, taken together, could form an M-element array, i.e. the meta-array [18]. At the lower level, each transmitting unit consists of a phased array of P colocated elements [18]. Through exploiting flexible waveform design, the HMPAR can achieve arbitrary transmit beampatterns while retaining phased-array-like resolution on receive [16], [17]. The signaling strategies of the notional HMPAR architecture to achieve various transmit beampatterns was developed in [18], and a target localization algorithm was provided in [19]. In [20], a similar radar concept that is called the phased-MIMO radar, in which the partitioned subarrays are allowed to overlap, was proposed. It was shown that the phased-MIMO radar enjoyed better beampattern and signal-to-interference-plus-noise ratios (SINRs) performances when compared with conventional phased-array and MIMO radars. Later, the phased-MIMO radar was extended into the transmit beamspace (TB)-based MIMO radar concept, which focuses the energy of multiple transmitted orthogonal waveforms within a certain spatial sector using beamspace design techniques in [4], [21]. However, it is worth noting that, for the Phased-MIMO radar, the power management when an element is part of two (or more) different sub-arrays is not easy in the engineering realization. Recently, a novel technique for optimizing the performance of a hybrid phased-MIMO radar in the presence of strong jamming effects was proposed in [22]. In the hybrid phased-MIMO radar, two orthogonal waveforms beam-formed by coherent operation of two sub-arrays are used to combine the advantages of both colocated MIMO and PA radars simultaneouly.

It is worth noting that aforementioned studies, including the HMPAR, phased-MIMO, TB-based MIMO and hybrid phased-MIMO radars, are associated with the colocated MIMO radar. These hybrid concepts mainly focus on the signal design to achieve flexible transmit beampatterns. On the contrary, the study of combining the distributed MIMO radar and the PA radar is far from enough. In fact, the distributed MIMO radar does have many merits, such as spatial diversity gains and resolution improvement. In [23], a general MIMO radar configuration where both the transmitter and receiver have several well-separated sub-arrays with each sub-array containing closely spaced antennas was introduced, and an iterative generalized-likelihood ratio test (iGLRT) algorithm for target detection and parameter estimation was also proposed and numerically demonstrated using the linear

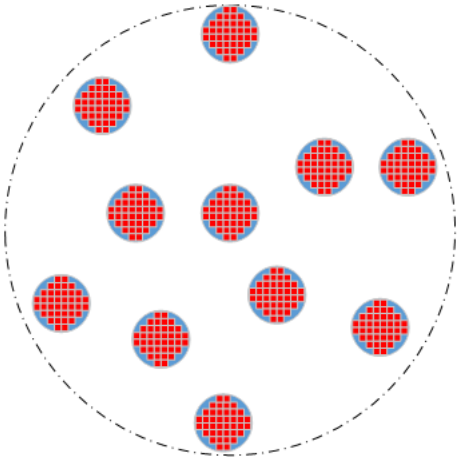

FIGURE 1. The system concept of hybrid distributed MIMO radar.

array configuration. Later, a notional MIMO radar system consisting of widely distributed phased arrays was proposed and studied in [24]. The distributed phased arrays consist of 5 uniform linear arrays (ULA) of 48 omnidirectional elements at half-wavelength spacing. The sub-arrays are spaced with their phase centers separated by 500 wavelengths. Therefore, this radar concept can be seen as a simplified hybrid distributed MIMO radar. In this paper, some preliminary simulations of transmit beampatterns and maximum-likelihood position estimations were presented. It was pointed out that, for the proposed distributed phased arrays, the coherent processing may not be desirable. However, since the lack of necessary theoretical analyses and detailed simulation parameters, the work presented in [24] is not very comprehensive and convincible. This motivates us to further study the hybrid distributed MIMO radar, which combines the distributed MIMO radar and the PA radar with more general configurations.

In this paper, we consider a particular hybrid distributed MIMO radar concept using T/R reciprocal antennas. As shown in Fig.1, the Hybrid distributed MIMO radar is composed of K sub-arrays which are randomly distributed with wide enough separations. Each sub-array consists of Q all-digital colocated antenna elements with T/R modules separated by half-wavelength inter-element spacing. The whole number of elements of this Hybrid MIMO is $M = K \times Q$. In the transmitting end, each sub-array operates as a PA radar and steers the transmit beam to cover the sector of interest where the desired target is likely to appear. Moreover, each sub-array is driven by an independent waveform that is orthogonal with waveforms transmitted by other sub-arrays. In the receiving end, the reflected signals are received by all elements in the whole array and jointly processed.

The proposed hybrid distributed MIMO radar offers a tradeoff between the PA radar and the distributed MIMO radar. This implies that:

1) Different sub-arrays viewing the target from different angles provide the possibility of exploiting spatial

diversity gains. This can be applied to overcome the target's RCS scintillation and achieve a reliable detection of spatial fluctuating targets.

2) The aperture size of each sub-array is smaller than that of the PA radar with the same number of elements, thus the transmit beam is relatively wide, which leads to wide surveillance coverage and long dwell time at the price of transmit coherent gain losses.

3) The whole array is applied to receive the reflected signal, thus high resolution can be obtained using jointly processing.

4) The number of orthogonal waveforms needed is equal to the number of sub-arrays, and thus much less orthogonal waveforms are needed as compared to the distributed MIMO radar.

For a radar system, two of most important issues are the target detection and localization [25]. As the first stage of resolving these two problems, here we intend to develop the optimal detection theory and the ambiguity function (AF) for the hybrid distributed MIMO radar.

In [26], the spatial diversity was exploited to improve detection performance of fluctuating targets for the distributed MIMO radar. The optimal detector in Neyman-Pearson sense was developed and the optimal detection performance was evaluated using the concept of 'detector's signal-to-noise ratio (SNR)'. In [27], the relative entropy was introduced to evaluate the optimal detection performance for MIMO radar. In [28], the likelihood ratio test (LRT) detector was developed and optimization problems were discussed for a novel multisite radar system (MSRS) with MIMO radars, i.e., MIMO-MSRS system. To confirm the better detection of fluctuating targets for MIMO radar systems, numerical and experimental studies incorporating realistic RCS properties were performed in [29].

The AF that was first developed by Woodward in [30] is a useful tool to study the localization problem of radar systems [4], [8]. For MIMO radar systems, the AF expressions were extended based on the optimum detection theory in [31], [32] and based on the log-likelihood function in [33], [34]. In fact, these two approaches are inherently equivalent. Recently, some new definitions of MIMO radar AF associated with the information theory are introduced in [35], [36]. Moreover, the properties of MIMO radar AF were studied and used to optimize the waveform design in [37]–[39].

In this paper, we develop the signal model of the proposed hybrid distributed MIMO radar considering its unique system configuration and using the spatial Swerling-I target model [40]. For the target detection problem, the optimal detector in Neyman-Pearson sense is derived and, the detection performance is evaluated using the receiver operating characteristic (ROC) curve and the relative entropy. For the target localization problem, the AF is derived for the hybrid distributed MIMO radar, based on the optimal detection principle. It will be shown that the hybrid MIMO radar AF is a general AF definition for the distributed MIMO radar and the PA radar.

The rest of this paper is organized as follows. In section II, the preliminary theory of MIMO radar is presented and the signal model of the hybrid distributed MIMO radar is developed. In section III, aiming at the optimal detection of fluctuating targets, we derive the optimal detector in Neyman-Pearson sense and evaluate its performance. In section IV, the AF is developed for the hybrid distributed MIMO radar based on the optimal detection principle, and the relationships between the hybrid distributed MIMO radar AF and the existing several AFs are discussed. Several numerical examples are presented to validate the effectiveness of the proposed hybrid MIMO radar in section V. Finally, conclusions and future work are drawn in section VI.

II. THEORETICAL BACKGROUND AND SIGNAL MODEL

In this section, we firstly present the preliminary theory of the traditional MIMO radar, and then develop the signal model of the proposed hybrid distributed MIMO radar in a concise form, with considering its system characteristics.

A. PRELIMINARY THEORY OF MIMO RADAR

Let us consider a general MIMO radar system with M transmitting elements and N receiving elements.The position coordinate of the i th transmitting element is $\mathbf{T}_i = (x_{ti}, y_{ti}, z_{ti})$, and that of the jth receiving element is $\mathbf{R}_j = (x_{rj}, y_{rj}, z_{rj})$. Then the position vectors of the transmitting and receiving arrays are

$$\mathbf{T} = [\mathbf{T}_1, \mathbf{T}_2, \ldots, \mathbf{T}_M] \tag{1}$$

$$\mathbf{R} = [\mathbf{R}_1, \mathbf{R}_2, \ldots, \mathbf{R}_N] \tag{2}$$

The signal transmitted from the ith transmitting element is

$$s_{ti}(t) = \sqrt{E/M} \cdot s_i(t) \cdot \exp[j2\pi f_c t] \tag{3}$$

where E is the total average transmitted energy, t denotes the time variable, f_c is the carrier frequency, and $s_i(t)$ is the signal envelope and satisfies the ideal orthogonal assumption

$$\int s_i(t) \cdot s_{i'}^*(t)\mathrm{d}t = \begin{cases} 1, & i = i'; \\ 0, & i \neq i'. \end{cases} \tag{4}$$

For a target in the observed region, we assume that its position vector is $\mathbf{P}$, its velocity vector is $\mathbf{V}$, and its scattering coefficient in the (i, j)th transmit-receive channel is ζ_{ji}, respectively. To get a concise expression in the following derivation, we use a parameter vector $\mathbf{\Theta} = [\mathbf{P}; \mathbf{V}]$ to describe the target. The position and velocity vectors are defined in the same coordinate system as the transmitting and receiving arrays. Therefore, the two-way time delay of the target located at position $\mathbf{P}$ associated with the (i, j)th transmit-receive channel can be written as

$$\tau_{ij}(\mathbf{P}) = \tau_i(\mathbf{P}) + \tau_j(\mathbf{P}) = \frac{\|\mathbf{P} - \mathbf{T}_i\|}{c} + \frac{\|\mathbf{P} - \mathbf{R}_j\|}{c} \tag{5}$$

where c is the light speed, and $\|\cdot\|$ is the Euclidean vector norm [31].

Similarly, for the transmit-receive channel, the Doppler frequency of the moving target with velocity $\mathbf{V}$ can be given by

$$\begin{aligned} f_{d,ij}(\mathbf{\Theta}) &= f_{d,i}(\mathbf{\Theta}) + f_{d,j}(\mathbf{\Theta}) \\ &= \frac{1}{\lambda} \cdot \left\langle \frac{\mathbf{P}-\mathbf{T}_i}{\|\mathbf{P}-\mathbf{T}_i\|}, \mathbf{V} \right\rangle + \frac{1}{\lambda} \cdot \left\langle \frac{\mathbf{P}-\mathbf{R}_j}{\|\mathbf{P}-\mathbf{R}_j\|}, \mathbf{V} \right\rangle \end{aligned} \quad (6)$$

where λ is the wavelength, and $\langle \cdot, \cdot \rangle$ is the inner product operator [32].

In the receiving end, the signal received by the jth receiving element, after demodulation, can be given by

$$\begin{aligned} r_j(t) = \sqrt{E/M} \cdot \sum_{i=1}^{M} \zeta_{ji} \cdot s_i\left(t - \tau_{ij}(\mathbf{P})\right) \exp\left[j2\pi f_{d,ij}(\mathbf{\Theta})t\right] \\ \cdot \exp\left[-j2\pi\, \tau_{ij}(\mathbf{P})(f_c + f_{d,ij}(\mathbf{\Theta}))\right] + n_j(t) \end{aligned} \quad (7)$$

where $n_j(t)$ denotes the background noise at the jth receiving antenna [29].

B. SIGNAL MODEL OF HYBRID DISTRIBUTED MIMO RADAR

For the hybrid distributed MIMO radar, the signal model given by (7) can be rewritten to get a concise matrix form, considering of its system configuration characteristics. First of all, the number of transmitting elements is equal to that of the receiving elements, i.e. $M = N$. Furthermore, we define the following denotations

$$\begin{aligned} a_j &= \exp\left[-j2\pi f_c \tau_j(\mathbf{P})\right] \\ b_i &= \exp\left[-j2\pi f_c \tau_i(\mathbf{P})\right] \\ \alpha_{ji} &= \zeta_{ji} \cdot \exp\left[-j2\pi f_{d,ij}(\mathbf{\Theta})\tau_{ij}(\mathbf{P})\right] \\ d_{ji}(t) &= \exp\left[j2\pi f_{d,ij}(\mathbf{\Theta})t\right] \end{aligned} \quad (8)$$

Then the signal received by the the j th receiving element can be rewritten as

$$r_j(t) = \sqrt{E/M} \cdot \textstyle\sum_{i=1}^{M} \alpha_{ji} a_j b_i d_{ji}(t) s_i\left(t - \tau_{ij}(\mathbf{P})\right) + n_j(t) \quad (9)$$

where a_j is the jth element in the receiver steering vector $\mathbf{a}$, b_i is the ith element in the transmitter steering vector $\mathbf{b}$, α_{ji} is the jith element of the extended channel matrix $\mathbf{H}$, i.e. $[\mathbf{H}]_{ji} = \alpha_{ji}$, $d_{ji}(t)$ is the ji th element of the Doppler phase matrix $\mathbf{D}(t)$, i.e., $[\mathbf{D}]_{ji} = d_{ji}(t)$, respectively.

To get a concise form of the signal model, some simplifications should be reasonably made based on the unique system configuration of the hybrid distributed MIMO radar. As mentioned before, the hybrid distributed MIMO radar is composed of K widely separated sub-arrays, and each sub-array is formed with Q closely spaced elements. Therefore, for an arbitrary sub-array, some approximations of the receiver/transmitter steering vectors, the extended channel matrix and the Doppler phase matrix can be made. Firstly, the elements within an arbitrary sub-array are close enough to each other so that for a target located in the far-field, the Line-of-Sight (LOS) of these elements is nearly identical. Therefore, for an arbitrary sub-array, the scattering coefficients of the target for its elements can be reasonably assumed to be fixed. Furthermore, for a moving target, the projection of the velocity vector onto the LOS of each element within an arbitrary sub-array is nearly identical. This implies that all the elements in an arbitrary sub-array might see nearly same frequency shifts for a moving target. Finally, we assume that narrow-band signal is applied in the hybrid distributed MIMO radar, and then the effect of the time delay on the signal envelope is almost the same for all elements in an arbitrary sub-array [31]. Based on these assumptions, the receiver/transmitter steering vectors can be rewritten as block vectors

$$\begin{aligned} \mathbf{a} &= \left[\mathbf{a}_1^T, \ldots, \mathbf{a}_p^T, \ldots, \mathbf{a}_K^T\right]^T, \quad \mathbf{a}_p = \left[a_{p1}, a_{p2}, \ldots, a_{pQ}\right]^T \\ \mathbf{b} &= \left[\mathbf{b}_1^T, \ldots, \mathbf{b}_q^T, \ldots, \mathbf{b}_K^T\right]^T, \quad \mathbf{b}_q = \left[b_{q1}, b_{q2}, \ldots, b_{qQ}\right]^T \end{aligned} \quad (10)$$

where $\mathbf{a}_p$ is the receiver steering vector of the pth sub-array and the $\mathbf{b}_q$ is the transmitter steering vector of the qth sub-array, respectively. The extended channel matrix and the Doppler phase matrix can be expressed as block matrices

$$\begin{aligned} [\mathbf{H}]_{pq} &= \alpha_{pq} \cdot \mathbf{1}_{QQ}, \quad p, q = 1, 2, \ldots, K \\ [\mathbf{D}]_{pq} &= d_{pq}(t) \cdot \mathbf{1}_{QQ}, \quad p, q = 1, 2, \ldots, K \end{aligned} \quad (11)$$

where α_{pq} denotes the extended scattering coefficient in the pqth observing channel (the qth sub-array acts as the transmitter, and the pth sub-array acts as the receiver), $d_{pq}(t)$ denotes the Doppler phase term in the pq th observing channel, respectively, and $\mathbf{1}_{QQ}$ is the all-one matrix with $Q \times Q$ elements.

In the hybrid distributed MIMO radar, sub-arrays are randomly distributed with wide separations, which implies that different sub-arrays observe the target from different aspects. Moreover, it is assumed that the observed target conforms to the Swerling-I model [40]. Therefore, α_{pq} is independent with each other and the distribution of $\boldsymbol{\alpha} = [\alpha_{11}, \ldots, \alpha_{1K}, \alpha_{21}, \ldots, \alpha_{KK}]$ is

$$\boldsymbol{\alpha} \sim CN\left(0, \mathbf{I}_{K^2}\right) \quad (12)$$

where $\mathbf{I}_{K^2}$ is the identity matrix with $K^2 \times K^2$ elements, $CN(\cdot, \cdot)$ is the complex normal distribution. Further, the probability density function of $\boldsymbol{\alpha}$ can be given by

$$p(\boldsymbol{\alpha}) = c_1 \cdot \exp\left[-\|\boldsymbol{\alpha}\|^2\right] \quad (13)$$

where c_1 is a normalized constant.

In the transmitting end, each sub-array operates in the PA radar mode, thus all the elements in each sub-array transmit fully correlated waveforms. Therefore, the transmit signal can be expressed as a block vector

$$\mathbf{s}(t) = \left[\mathbf{w}_1^T s_1(t), \ldots, \mathbf{w}_q^T s_q(t), \ldots, \mathbf{w}_K^T s_K(t)\right]^T \quad (14)$$

where $\mathbf{w}_q$ is the beamforming weight vector and $s_q(t)$ is the transmitted signal for the qth sub-array, respectively. Moreover, since each sub-array transmits as a PA radar, the transmit coherent gain for the qth sub-array can be realized by taking $\mathbf{b}_q = \mathbf{w}_q$, i.e., $\mathbf{b}_q^H \mathbf{w}_q = Q$.

Finally, the received signal of the hybrid distributed MIMO radar can be formed into a block vector

$$\mathbf{r}(t) = \left[\mathbf{r}_1^T, \ldots, \mathbf{r}_p^T, \ldots, \mathbf{r}_K^T\right]^T \tag{15}$$

where the received signal vector of the pth sub-array is

$$\begin{aligned}\mathbf{r}_p(t) &= \sqrt{E/M} \cdot \sum_{q=1}^{K} \alpha_{pq}\mathbf{a}_p\mathbf{b}_q^H\mathbf{w}_q d_{pq}(t)s_q(t-\tau_{pq}) + \mathbf{n}_p(t) \\ &= \sqrt{E/M} \cdot Q \cdot \sum_{q=1}^{K} \alpha_{pq}\mathbf{a}_p d_{pq}(t)s_q(t-\tau_{pq}) + \mathbf{n}_p(t)\end{aligned} \tag{16}$$

where $\mathbf{n}_p(t) = \left[\mathbf{n}_{p1}(t), \ldots, \mathbf{n}_{p2}(t), \ldots, \mathbf{n}_{pQ}(t)\right]^T$ is the noise vector associated with the p th sub-array, and its correlation matrix is $\sigma_n^2\mathbf{I}_Q$, σ_n^2 is the noise variance of each receiver element, $\mathbf{I}_Q$ is the identity matrix with Q×Q elements.

III. OPTIMAL DETECTOR AND ITS PERFORMANCE

In this section, we will refer to the optimal detection of the hybrid distributed MIMO radar, including the derivation of the optimal detector in the Neyman-Pearson sense and the distribution of statistics. Furthermore, the best achievable detection performance will be evaluated using the concept of relative entropy, followed by some comparisons between the optimal detection performance of the hybrid distributed MIMO radar and that of the traditional MIMO and PA radars.

A. OPTIMAL DETECTOR IN THE NEYMAN-PEARSON SENSE

Generally, the radar detection problem can be treated as a binary hypothesis test. Among many detection theories, the optimal detector in the Neyman-Pearson sense, which maximizes the detection probability given that the probability of false alarm is fixed, is the most frequently-used one. Assuming that the target status parameter $\mathbf{\Theta}$ and the noise variance σ_n^2 are known, the optimal detector in the Neyman-Pearson sense is the Likelihood Ratio Test (LRT),

$$T = \frac{f\left(\mathbf{r}(t)|\mathcal{H}_1\right)}{f\left(\mathbf{r}(t)|\mathcal{H}_0\right)} \underset{<\mathcal{H}_0}{>^{\mathcal{H}_1}} \delta_0 \tag{17}$$

where $f\left(\mathbf{r}(t)|\mathcal{H}_1\right)$ and $f\left(\mathbf{r}(t)|\mathcal{H}_0\right)$ are the likelihood functions under two hypotheses, and δ_0 is the threshold. The binary hypotheses are

$\mathcal{H}_1$:Target exists with status parameter $\mathbf{\Theta}$;

$\mathcal{H}_0$:Target does not exist with status parameter $\mathbf{\Theta}$.

According to (15) and (16), the received signals of each sub-array have the same expressions. Without the loss of generality, the received signals of an arbitrary sub-array (e.g., the pth sub-array) under different hypotheses can be given as

$$\mathbf{r}_p(t) = \begin{cases}\mathbf{s}_p(t) + \mathbf{n}_p(t), & \mathcal{H}_1\,; \\ \mathbf{n}_p(t), & \mathcal{H}_0\,.\end{cases} \tag{18}$$

where

$$\mathbf{s}_p(t) = \sqrt{E/M} \cdot Q \cdot \sum_{q=1}^{K} \alpha_{pq}\mathbf{a}_p d_{pq}(t)s_q(t-\tau_{pq}) \tag{19}$$

Therefore, under the null hypothesis, the probability density function (PDF) of the received signals $\mathbf{r}(t)$ can be given by

$$f\left(\mathbf{r}(t)|\mathcal{H}_0\right) = c_2 \cdot \exp\left[-\frac{\int\|\mathbf{r}(t)\|^2\mathrm{d}t}{\sigma_n^2}\right] \tag{20}$$

Under the alternative hypothesis, after some tedious mathematical derivations (see Appendix A), the PDF of the received measurements can be given by

$$\begin{aligned}f\left(\mathbf{r}(t)|\mathcal{H}_1\right) &= \int f\left(\mathbf{r}(t)|\mathcal{H}_1, \boldsymbol{\alpha}\right) p(\boldsymbol{\alpha}) d\boldsymbol{\alpha} \\ &= c_3 \cdot \exp\left[-\frac{\int\|\mathbf{r}(t)\|^2\mathrm{d}t}{\sigma_n^2} + \frac{\frac{EQ^2}{M}\|\mathbf{X}\|^2}{\sigma_n^2\left(\sigma_n^2 + \frac{EQ^3}{M}\right)}\right]\end{aligned} \tag{21}$$

where c_2 and c_3 are normalized constants that are negligible in the following derivations, $\mathbf{x} = [x_{11}, \ldots, x_{1K}, x_{21}, \ldots, x_{KK}]$ is the output of a bank of matched filters and

$$\|\mathbf{X}\|^2 = \sum_{p=1}^{K}\sum_{q=1}^{K}|x_{pq}|^2 \tag{22}$$

where

$$x_{pq} = \int \mathbf{a}_p^H\mathbf{r}_p(t)d_{pq}^*(t)s_q^*(t-\tau_{pq})\mathrm{d}t \tag{23}$$

It should be pointed out that the assumption of $\mathbf{b}_q = \mathbf{w}_q$ was applied in the above derivation, i.e., $\mathbf{b}_q^H\mathbf{w}_q = Q$. This implies that the beamforming direction is exactly pointing to the desired target, and then the best detection can be achieved.

Therefore, the optimal detector of the hybrid distributed MIMO radar in the Neyman-Pearson sense can be given by

$$T = \|\mathbf{X}\|^2 \underset{<\mathcal{H}_0}{>^{\mathcal{H}_1}} \delta \tag{24}$$

where the threshold δ depends on the FA probability.

For MIMO radar, all the information of receive signal should be considered together to achieve the optimal detection. However, as shown in (22) and (24), we only need to send the output of a bank of matched filters to a "decision module". In this way, the cost of the data transmission is not very high.

B. DISTRIBUTION OF STATISTICS

In this sub-section, we further derive the distribution of statistics based on the optimal detector expression given by (24). To evaluate the best acheivable detection performance, we assume that the effect of the Doppler frequency shift is negligible or the Doppler frequency shift is perfectly matched, i.e., $d_{pq}(t) = 1$.

Under the null hypothesis,

$$x_{pq} = \mathbf{a}_p^H \int \mathbf{n}_p(t)s_q^*(t-\tau_{pq})\mathrm{d}t = n_{pq} \tag{25}$$

The noise is independent with the signal and $\mathbf{n}_p(t)$ is a zero-mean complex Gaussian white noise with the variance of σ_n^2,

therfore, the output of matched filter n_{pq} is still a zero-mean complex Gaussian white noise and, $n_{pq} \sim CN\left(0, Q\sigma_n^2\right)$.

Under the alternative hypothesis,

$$\begin{aligned} x_{pq} &= Q^2\sqrt{\frac{E}{M}} \cdot \alpha_{pq} \int s_q(t-\tau_{pq}) s_q^*(t-\tau_{pq}) \mathrm{d}t \\ &\quad + \mathbf{a}_p^H \int \mathbf{n}_p(t) s_q^*(t-\tau_{pq}) \mathrm{d}t \\ &= Q^2\sqrt{\frac{E}{M}} \cdot \alpha_{pq} + n_{pq} \end{aligned} \tag{26}$$

where $\int s_q(t-\tau_{pq}) s_q^*(t-\tau_{pq}) \mathrm{d}t = 1$ is applied. As mentioned before, α_{pq} is a zero-mean complex Gaussian random variable, thus the output of matched filter n_{pq} is still a zero-mean complex Gaussian and, $x_{pq} \sim CN\left(0, \frac{Q^4E}{M} + Q\sigma_n^2\right)$.

The optimal detetor statistics of the hybrid distributed MIMO radar $\|\mathbf{X}\|^2$ is the quadratic sum of K^2 independent zero-mean, equal variance, complex Guassian random variables, thus its distribution can be given by

$$T = \|\mathbf{X}\|^2 \sim \begin{cases} \left(\frac{Q^4E}{2M} + \frac{Q\sigma_n^2}{2}\right) \cdot \chi^2_{2K^2}, & \mathcal{H}_1\,; \\ \frac{Q\sigma_n^2}{2} \cdot \chi^2_{2K^2}, & \mathcal{H}_0\,; \end{cases} \tag{27}$$

where χ_d^2 is the chi-square distribution with d degrees of freedom.

C. DETECTION PERFORMANCE

In this sub-section, we will evaluate the performance of the derived LRT detector of the hybrid distributed MIMO radar, using two useful performance measures. One of these is the Receiver Operating Characteristic (ROC) curve, another one is the upper bound of the detection performance.

1) ROC CURVE

In the radar detection theory, the ROC curve is created by plotting the probability of detection P_D against the probability of false alarm P_{FA}. Usually, the ROC curve represents the inherent trade-off between sensitivity and specificity of a detector. Based on (27), the probability of false alarm, the threshold and the probability of detection of the hybrid MIMO radar can be derived. Firstly, the probability of false alarm is given by

$$\begin{aligned} \mathrm{P}_{FA} &= \Pr(T > \delta | \mathcal{H}_0) \\ &= \Pr\left(\frac{Q\sigma_n^2}{2} \cdot \chi^2_{2K^2} > \delta\right) \\ &= \Pr\left(\chi^2_{2K^2} > \frac{2\delta}{Q\sigma_n^2}\right) \end{aligned} \tag{28}$$

where $\Pr(\cdot)$ denotes the cumulative distribution function (CDF) operator.

Further, we can get the threshold

$$\delta = \frac{Q\sigma_n^2}{2} \cdot F^{-1}_{\chi^2_{2K^2}}(1 - \mathrm{Pr}_{FA}) \tag{29}$$

where $F^{-1}_{\chi^2_{2K^2}}(\cdot)$ denotes the inverse CDF of a chi-square random variable with $2K^2$ degrees of freedom [42]. Finally, the probability of detection can be expressed as

$$\begin{aligned} \mathrm{P}_D &= \Pr(T > \delta | \mathcal{H}_1) \\ &= \Pr\left(\left(\frac{Q^4E}{2M} + \frac{Q\sigma_n^2}{2}\right) \chi^2_{2K^2} > \delta\right) \\ &= 1 - F_{\chi^2_{2K^2}}\left(\frac{2\delta}{Q^4E/M + Q\sigma_n^2}\right) \end{aligned} \tag{30}$$

According to (29), the ROC curve of the optimal detector of the hybrid MIMO radar can be given by

$$\mathrm{P}_D = 1 - F_{\chi^2_{2K^2}}\left(\frac{1}{Q^3\rho/M + 1} \cdot F^{-1}_{\chi^2_{2K^2}}(1 - \mathrm{P}_{FA})\right) \tag{31}$$

where $\rho = E/\sigma_n^2$ represents the SNR level of the hybrid MIMO radar, $F_{\chi^2_{2K^2}}$ denotes the CDF of a chi-square random variable with $2K^2$ degrees of freedom. In the section V, ROC curves with different system configurations and parameters will be presented and further discussed.

2) UPPER BOUND OF THE DETECTION PERFORMANCE

Another measure of a detector is the upper bound of detection performances. To evaluate the detection performance of the distributed MIMO radar, a index named 'detector's SNR', which is equivalent to the 'divergence' in [42], was introduced in [26]. Using the concept of 'detector's SNR', the detection performances of the statistical MIMO radar, traditional PA radar and multi-input single-output (MISO) radar were presented and compared. Later, the concept of relative entropy in the information theory was introduced to measure the detection performance of the MIMO radar in [27]. Since the 'detector's SNR' can be seen as a special case of the relative entropy in the Gaussian assumption [27], hereafter we use the relative entropy to measure the upper bound of the detection performance of the hybrid MIMO radar.

According to the Stein lemma, the best achievable detection performance is bounded by the relative entropy that is defined as [43]

$$\mathrm{D}(P_0 \| P_1) = \int P_0(x) \cdot \frac{P_0(x)}{P_1(x)} dx \tag{32}$$

where P_0 and P_1 are the probability density functions (PDF) of the statistic under the null and alternative hypotheses, respectively.

Based on (27), the upper bound of the detection performance of the hybrid distributed MIMO radar can be given by

$$\begin{aligned} \mathrm{D}_{HM} &= \int \Gamma(K^2, Q\sigma_n^2) \cdot \ln\left(\frac{\Gamma(K^2, Q\sigma_n^2)}{\Gamma(K^2, Q\sigma_n^2 + Q^4E/M)}\right) \mathrm{d}t \\ &= K^2 \cdot \left(\ln\left(1 + \frac{\rho Q^3}{M}\right) - \frac{\rho Q^3}{M + \rho Q^3}\right) \end{aligned} \tag{33}$$

where $\Gamma(\cdot,\cdot)$ denotes the Gamma distribution function, the detailed derivation of (33) can be found in Appendix B.

D. DISCUSSION

In this sub-section, we further discuss the derived optimal detection theory of the hybrid distributed MIMO radar, including its relationships with other radar systems, and its effect on system configurations.

As previously mentioned, the hybrid distributed MIMO radar serves as a compound of the distributed MIMO and PA radars. Therefore, compared with the works in [25]–[27], the derived optimal detector is a more general expression. In some special cases, the derived optimal detector can degrade into existing expressions for the distributed MIMO and PA radars.

1) RELATIONSHIPS WITH OTHER RADAR SYSTEMS

If the number of sub-array K is decreased to 1, and $Q = M$, then the hybrid distributed MIMO radar will degrade into the traditional PA radar. If the number of sub-array K is increased to M, and $Q = 1$, then the hybrid distributed MIMO radar will degrade into the traditional distributed MIMO radar.

The detailed discusstions can be seen in Appendix C.

2) EFFECT OF SNR ON DETECTION PERFORMANCES

As presented in (33), the relative entropy of the hybrid distributed MIMO radar is related to the system SNR ρ. Therefore, the effect of SNR on the best achievable detection performance should be properly studied.

For the case of high SNR, i.e., ρ is very large, the relative entropy of the hybrid distributed MIMO radar can be rewritten as

$$\mathrm{D}_{HM} = K^2 \cdot \left(\ln\left(1 + \frac{\rho M^2}{K^3}\right) - 1 \right) \tag{34}$$

where $M = K \times Q$ is applied. It can be seen that, in the high SNR case, the optimal detection performance improves with the increasement of the number of sub-arrays.

Similarly, for the case of low SNR, i.e., ρ is very small, the relative entropy of the hybrid distributed MIMO radar can be rewritten as

$$\mathrm{D}_{HM} \approx \frac{1}{2} \cdot \left(\frac{M}{K}\right)^2 \cdot \rho^2 \tag{35}$$

It can be seen that, on the contrary, the optimal detection performance improves with the decrement of the number of sub-arrays in the low SNR case.

These conclusions of the hybrid distributed MIMO radar are also coincident with the results presented in [26], [27]. For high SNR, the distributed MIMO radar provides better detection performance than the PA radar. In this case, even though the PA radar can enjoy the coherent processing gain, it may also encounter very low received power with non-negligible probability due to the target fluctuation. On the other hand, the distributed MIMO radar can be seen as plenty of independent radar systems. Therefore, it can exploit spatial diversity by viewing the target from different aspects to overcome the target fluctuation. For low SNR, in contrast, the PA radar provides better detection performance than the distributed MIMO radar. In this case, the PA radar's disadvantage becomes its advantage. When the transmitted power is low, the PA radar may still achieve relative high received power with nonnegligible probability, since the target is spatially fluctuating. However, the distributed MIMO radar does not enjoy this benefit.

In this paper, for the case of small number of sub-arrays, the hybrid distributed MIMO radar tends to the traditional PA radar configuration. In this case, the hybrid distributed MIMO radar can achieve better detection performance for fluctuating targets with low SNR. While for the case of larger number of sub-arrays, the hybrid distributed MIMO radar tends to the distributed MIMO radar configuration. Therefore, the hybrid distributed MIMO radar system mainly enjoys the spatial diversity gain, and achieves better detection performance for fluctuating targets with high SNR.

IV. AMBIGUITY FUNCTION

As a useful theoretical tool, AF has been deeply studied and widely applied in many radar fields, such as waveform design, resolution measurement and system analysis. Up to now, the AF expressions have been extended for MIMO radar systems in [30]–[35]. Even though there are many different definitions of MIMO radar, the most popular and acceptable one is asscociated with the optimal detection concept and the matched filter theory. In this paper, without the loss of generality, we derive the AF of the hybrid distributed MIMO radar based on the above derived optimal detector.

A. AF DEFINITION OF THE HYBRID DISTRIBUTED MIMO RADAR

As given by (22), the optimal detector of the hybrid distributed MIMO radar is the square summation of the output of a bank of matched filters, and the output of arbitrary one matched filter is given by (23). In the following derivation, we assume that the received signal is associated with a point target (the ideal target) with the status parameter $\boldsymbol{\Theta}$ and, the matched filter is associated with another point target (the real target) with the status parameter $\boldsymbol{\Theta'}$. Omitting the negligible magnitude term and noise term, the output of arbitrary one matched filter can be written as (36), as shown at the bottom of the next page, where $\alpha_{pq} = 1$ is applied, i.e., the ideal point target is assumed in the derivation.

Letting that $\Delta\tau_{pq}(\boldsymbol{\Theta}, \boldsymbol{\Theta'}) = \tau_{pq}(\boldsymbol{\Theta}) - \tau_{pq}(\boldsymbol{\Theta'})$ and $\Delta f_{d,pq}(\boldsymbol{\Theta}, \boldsymbol{\Theta'}) = f_{d,pq}(\boldsymbol{\Theta}) - f_{d,pq}(\boldsymbol{\Theta'})$, the integration term in the last step in (36) can be rewritten as the well-known Woodward's AF

$$\chi_{pq}(\Delta\tau_{pq}, \Delta f_{d,pq}) = \int s_q(t) s_q^*(t - \Delta\tau_{pq}) \cdot \exp\left[j2\pi\, \Delta f_{d,pq} t\right] \mathrm{d}t \tag{37}$$

and (36) can be rewritten as

$$x_{pq}(\boldsymbol{\Theta}, \boldsymbol{\Theta'}) = \mathbf{a}_p^H(\boldsymbol{\Theta'}) \mathbf{a}_p(\boldsymbol{\Theta}) \mathbf{b}_q^H(\boldsymbol{\Theta}) \mathbf{w}_q(\boldsymbol{\Theta'}) \chi_{pq}(\Delta\tau_{pq}, \Delta f_{d,pq}) \tag{38}$$

According to the derived optimal detector presented in (22), the AF of the hybrid distributed MIMO radar is defined as the square summation of the output of matched filter that is associated with the 'pure' signal.

$$\begin{aligned}&\chi_{HM}(\boldsymbol{\Theta}, \boldsymbol{\Theta'})\\&=\sum_{p=1}^{K}\sum_{q=1}^{K}|x_{pq}(\boldsymbol{\Theta}, \boldsymbol{\Theta'})|^2\\&=\sum_{p=1}^{K}\sum_{q=1}^{K}|\mathbf{a}_p^H(\boldsymbol{\Theta'})\mathbf{a}_p(\boldsymbol{\Theta})|^2|\mathbf{b}_q^H(\boldsymbol{\Theta})\mathbf{w}_q(\boldsymbol{\Theta'})|^2|\chi_{pq}(\Delta\tau_{pq}, \Delta f_{d,pq})|^2\end{aligned} \tag{39}$$

where the first term $|\mathbf{a}_p^H(\boldsymbol{\Theta'})\mathbf{a}_p(\boldsymbol{\Theta})|^2$ and the second term $|\mathbf{b}_q^H(\boldsymbol{\Theta})\mathbf{w}_q(\boldsymbol{\Theta'})|^2$ denote the phase shift information associated to the relative target position and motion for the corresponding receiver and transmitter sub-arrays, respectively. Since each sub-array in the hybrid distributed MIMO radar operates with the PA mode, the first term and the second term in (39) also represent the receive coherent processing gain and the transmit coherent processing gain, respectively. The last term $|\chi_{pq}(\Delta\tau_{pq}, \Delta f_{d,pq})|^2$, denoting the auto-correlation of the transmitted waveforms with the time delay error and Doppler shift, is the traditional Woodward's AF for the bistatic radar configuration.

B. RELATIONSHIPS WITH OTHER SYSTEMS

It can be found from (39) that the hybrid distributed MIMO radar AF is a non-coherent summation of the bistatic PA radar AF. This expression reflects the unique system configuration of the hybrid MIMO radar. As a whole, the hybrid distributed MIMO radar is a distributed MIMO radar, while from the local viewpoint, each sub-array of the hybrid distributed MIMO radar is a relative small PA radars. Therefore, the hybrid distributed MIMO radar AF given in (39) serves as a general AF definition for different radar configurations.

If the number of sub-array K is decreased to 1, and $Q = M$, then the hybrid distributed MIMO radar will degrade into traditional PA radar. In this case, the hybrid distributed MIMO radar AF can be rewritten as

$$\chi_{PA}(\boldsymbol{\Theta}, \boldsymbol{\Theta'})=|\mathbf{a}^H(\boldsymbol{\Theta'})\mathbf{a}(\boldsymbol{\Theta})|^2|\mathbf{b}^H(\boldsymbol{\Theta})\mathbf{w}(\boldsymbol{\Theta'})|^2|\chi(\Delta\tau, \Delta f_d)|^2 \tag{40}$$

where $\mathbf{a}$ is the receiver steering vector, $\mathbf{b}$ is the transmitter steering vector, and $\mathbf{w}$ is the beamforming weight vector of the PA radar, respectively, and $|\chi(\Delta\tau, \Delta f_d)|^2$ is the traditional narrow-band Woodward's AF. In this case, the target is usually assumed to be in the far field, and the relative geometry between transceivers and the target can be described using the azimuth and elevation angles. Accordingly, the degraded AF expression shown in (40) is consistent with the one form defined in [4], [18] and [21].

If the number of sub-array K is increased to M, and $Q = 1$, then the hybrid distributed MIMO radar will degrade into the distributed MIMO radar. In this case, the hybrid distributed MIMO radar AF can be rewritten as

$$\begin{aligned}&\chi_{MIMO}(\boldsymbol{\Theta}, \boldsymbol{\Theta'})\\&=\sum_{j=1}^{M}\sum_{i=1}^{M}|a_j^H(\boldsymbol{\Theta'})a_j(\boldsymbol{\Theta})|^2|b_i^H(\boldsymbol{\Theta})b_i(\boldsymbol{\Theta'})|^2|\chi_{ji}(\boldsymbol{\Theta}, \boldsymbol{\Theta'})|^2\end{aligned} \tag{41}$$

where a and b have been defined in Section II, and $|\chi_{ji}(\boldsymbol{\Theta}, \boldsymbol{\Theta'})|^2$ is the traditional delay-Doppler AF between the ith transmitting element and the jth receiving element. It should be pointed out that the MIMO radar AF given in (41) is consistent with the one developed in [38]. It can be seen that the MIMO radar AF given in (41) takes into account not only the effect of waveforms, but also that of the system geometry configuration.

V. NUMERICAL EXAMPLES

In this section, we present several numerical results associated with the derived theoretical work and validate the effectiveness of the proposed hybrid distributed MIMO radar.

A. DETECTION EXAMPLES

Here we mainly focus on the optimal detection of a fluctuating target with the spatial Swerling-I model [40]. According to (31), for the hybrid distributed MIMO radar, the probability of detection is a function of the system configuration, SNR and the probability of false alarm (P_{FA}). In the first example, given that P_{FA} is fixed as 10^{-6}, we study the probability of detection (P_D) of the hybrid distributed MIMO radar with different system configurations versus SNR. Here, we assume that the total number of elements $M = 16$, and the number of sub-arrays is $K = [1, 2, 4, 8, 16]$. Note that the hybrid distributed MIMO radar degrades into the traditional PA radar and distributed MIMO radar when $K = 1$ and $K = 16$, respectively. The calculated P_D of the hybrid distributed MIMO radar versus SNR using (31) is shown

$$\begin{aligned}x_{pq}(\boldsymbol{\Theta}, \boldsymbol{\Theta'}) &= \int \mathbf{a}_p^H(\boldsymbol{\Theta'})\mathbf{r}_p(t, \boldsymbol{\Theta})d_{pq}^*(t, \boldsymbol{\Theta'})s_q^*(t-\tau_{pq}(\boldsymbol{\Theta'}))\mathrm{d}t\\&= \int \mathbf{a}_p^H(\boldsymbol{\Theta'})\exp\left[-j2\pi f_{d,pq}(\boldsymbol{\Theta'})t\right]s_q^*(t-\tau_{pq}(\boldsymbol{\Theta'}))\cdot\sum_{q=1}^{K}\mathbf{a}_p(\boldsymbol{\Theta})\mathbf{b}_q^H(\boldsymbol{\Theta})\mathbf{w}_q(\boldsymbol{\Theta'})\exp\left[j2\pi f_{d,pq}(\boldsymbol{\Theta})t\right]s_q(t-\tau_{pq}(\boldsymbol{\Theta}))\mathrm{d}t\\&= \mathbf{a}_p^H(\boldsymbol{\Theta'})\mathbf{a}_p(\boldsymbol{\Theta})\mathbf{b}_q^H(\boldsymbol{\Theta})\mathbf{w}_q(\boldsymbol{\Theta'})\cdot\int s_q(t-\tau_{pq}(\boldsymbol{\Theta}))s_q^*(t-\tau_{pq}(\boldsymbol{\Theta'}))\cdot\exp\left[j2\pi\left(f_{d,pq}(\boldsymbol{\Theta})-f_{d,pq}(\boldsymbol{\Theta'})\right)t\right]\mathrm{d}t\end{aligned} \tag{36}$$

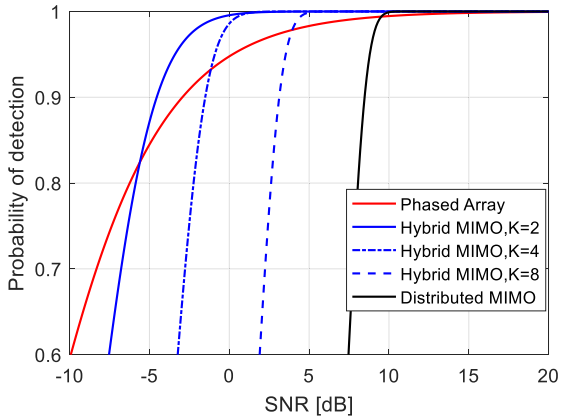

FIGURE 2. The probability of detection of the hybrid distributed MIMO radar with different configurations VS. SNR. The total number of elements M = 16 and the probability of false alarm $P_{FA} = 10^{-6}$.

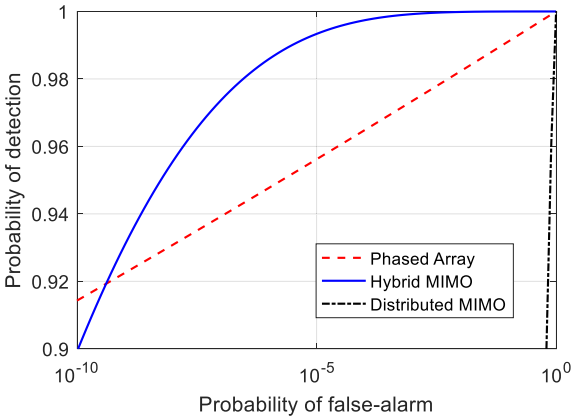

FIGURE 3. The ROC curves of the hybrid distributed MIMO radar (M = 16 and K = 4), the PA radar (M = 16 and K = 1) and the distributed MIMO radar (M = 16 and K = 16), respectively. The SNR is set to be 0dB.

in Fig.2. It can be found from this figure that, except for the low SNR region (smaller than −5.60 dB) where the PA radar achieves the highest P_D, the hybrid distributed MIMO radar benefits from the best detection performance. Note that the hybrid distributed MIMO radar with higher number of sub-arrays requires higher SNRs to achieve good detection performance. When the SNR is larger than 9.52dB, the P_D of the distributed MIMO radar (largest number of sub-arrays) becomes to outperform that of the PA radar. The reason for this is that, as presented in section III and [26], for the case of high SNR, the hybrid distributed MIMO radar with more number of sub-arrays can exploit more spatial diversity gains to achieve better detection performance. This will be further validated by the third example.

In our second example, we present ROC curves of the hybrid distributed MIMO radar. In this example, the total number of elements M is still chosen as 16, the number of sub-arrays K is fixed to be 4, and the SNR is chosen to be 0 dB. Fig.3 depicts the ROC curves of the hybrid MIMO radar with this particular system configuration. Meanwhile, the ROC curves of the PA radar ($K = 1$) and the distributed MIMO radar ($K = 16$) are presented, as well. It can be seen from this figure that the hybrid distributed MIMO radar is the best system to detect fluctuating targets over both the PA and distributed MIMO radars for most cases. Only when $P_{FA} < 4 \times 10^{-10}$, the PA radar enjoys higher P_D than the hybrid distributed MIMO radar.

The third example is conducted to show the best achievable detection performance of the hybrid distributed MIMO radar using relative entropy. According to (33), the relative entropy is only related to the system configuration and SNR. Here, the system configuration set of this example is the same as that of the first example, and the SNR varies from −20 dB to 20 dB. Fig.4 depicts the generated relative entropy. We can see from this figure that, the hybrid distributed MIMO radar enjoys the best detection performance for most SNR cases, while the PA radar is the optimal system for very low SNR (lower than −11.30 dB) and the distributed MIMO radar is

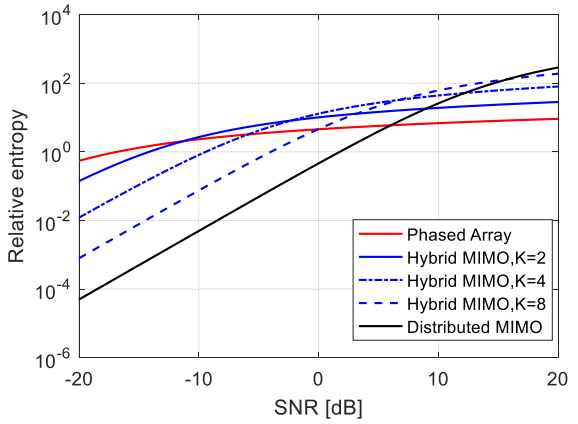

FIGURE 4. The Relative Entropy of the hybrid distributed MIMO radar with different configurations VS. SNR. The total number of elements M is set to be 16.

the best system for very high SNR (higher than 15.8dB). Note that, again, with the increase of SNR, the hybrid distributed MIMO radar with more number of sub-arrays provides better detection performance. This result is in accordance with the expectation. According to section III and [26], for the case of high SNR, it is better to use the hybrid distributed MIMO radar with more number of sub-arrays, while for the case of low SNR, it is better to use the hybrid configuration with less number of sub-arrays.

B. AMBIGUITY FUNCTION

Here we present the numerically generated AFs for the proposed hybrid distributed MIMO radar and also present comparisons to the PA and distributed MIMO radars. According to the developed AF definition, the AF of the hybrid distributed MIMO radar depends on the system configuration, transmitted waveform and target's status parameter. Therefore, in this paper, instead of presenting many AF examples for different cases, we present one typical hybrid MIMO radar AF example to show its unique resolution performance.

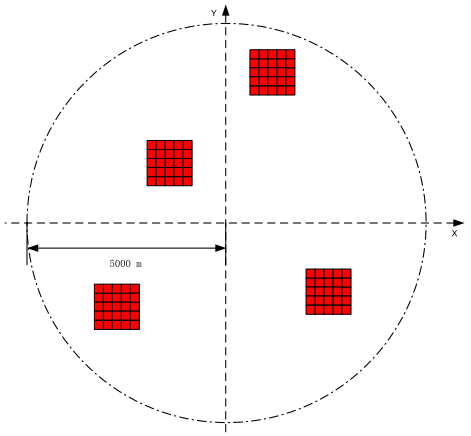

FIGURE 5. One realization of the system configurations of the hybrid distributed MIMO radar.

TABLE 1. Waveform parameters.

Parameters	Specification	Unit
Pulse number	5	-
Carrier frequency	9.95/10.00/10.05/10.10	GHz
Pulse duration	5	μs
Bandwidth	50	MHz
Pulse repetition frequency	10	KHz
Chirp rate	1×10^{13}	Hz/s
Time-bandwidth product	250	-

For the hybrid distributed MIMO radar, the total number of elements is selected to be 100, the number of sub-arrays is set to be 4, each sub-array is with 5 × 5 elements, and these sub-arrays are randomly distributed in a disk with a radius 5000m. Fig.5 illustrates one realization of this system configuration assumption. The frequency division multiple access (FDMA) waveforms are used in the simulation. Each sub-array transmits a train of Linear Frequency Modulation (LFM) pulses with different carrier frequencies. The specific parameters of the train of chirp pulses, as listed in the Table 1, are chosen to be the same as that used in [32]. The pulse number is 5, the pulse duration is 5μs, the bandwidth is 50MHz, and the pulse repetition frequency (PRF) is 10KHz. Accordingly, the chirp rate is 1×10^{13}Hz/s, and the time-bandwidth product is 250. The carrier frequency of each of four sub-arrays is set to be 9.95 GHz, 10.00GHz, 10.05GHz, and 10.10GHz, respectively.

Correspondingly, for the PA radar, the system configuration is set to be 10 × 10 elements, and the central position is located at the origin of the disk. The PA radar only needs one waveform, and thus the carrier frequency is set to be 10GHz, other parameters are set to be the same as before. For the distributed MIMO radar, 100 elements are assumed to be randomly located in the disk with radius 5000m. However, the generation of 100 OFDM waveforms is practically difficult and unnecessary for the calculation the distributed MIMO radar AF using (41). Here, for the sake of simplicity, we assume that each element transmit the same waveform as the PA radar and calculate the corresponding AFs.

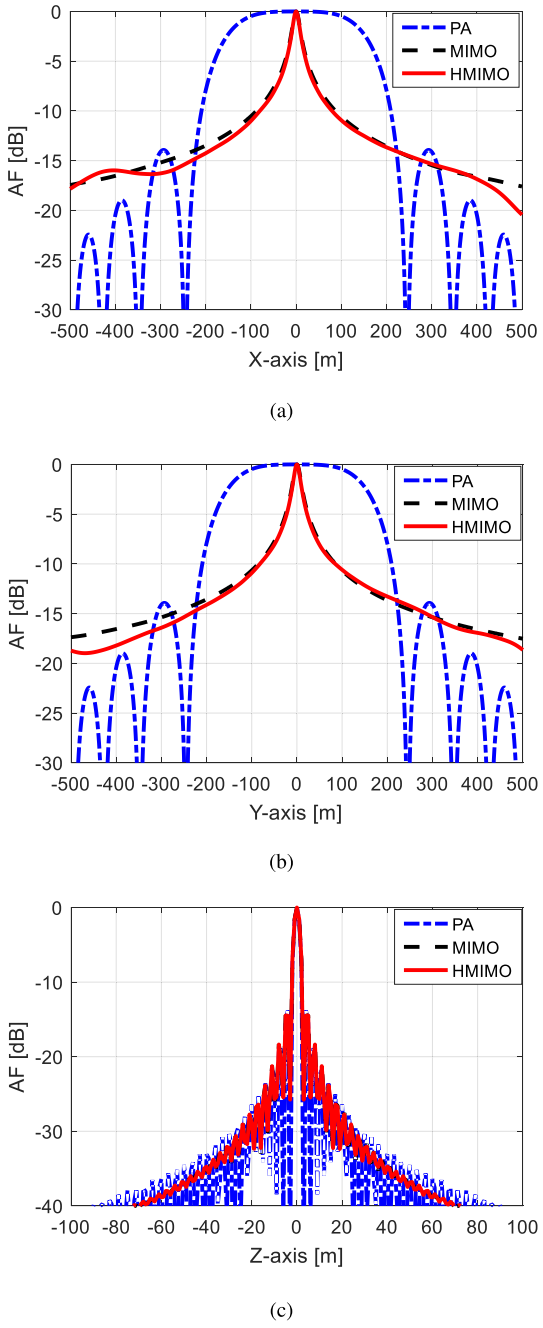

FIGURE 6. The Monte Carlo AFs of the Hybrid distributed MIMO radar, the PA radar and the distributed MIMO radar VS. position deviation along (a) X axis, (b) Y axis and (c) Z axis. For the hybrid distributed MIMO radar, the total number of elements is selected to be 100, the number of sub-arrays is set to be 4, each sub-array is with 5 × 5 elements, and these sub-arrays with are randomly distributed in a disk with a radius 5000m. The motionless target is assumed to be located at $[0m,0m,10000m]^T$.

Firstly, we consider a motionless target case, where the ideal target is located at $[0m,0m,10000m]^T$ and, the position parameter of the real target is chosen to be varying in the vicinity of that of the ideal target. In this case, the Doppler effect can be ignored, and only the position resolution is considered. Fig.6 depicts the numerical results. Note that, since the sub-arrays of the hybrid distributed MIMO radar are

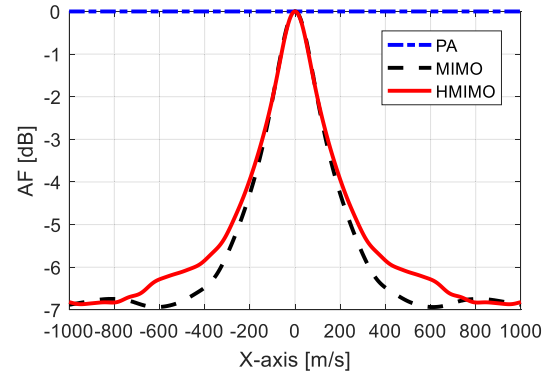

(a)

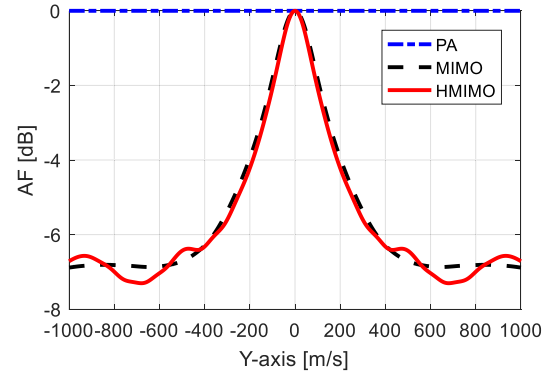

(b)

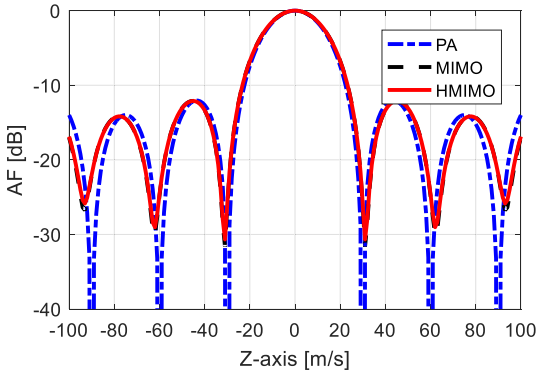

(c)

FIGURE 7. The Monte Carlo AFs of the Hybrid distributed MIMO radar, the PA radar and the distributed MIMO radar VS. velocity deviation along (a) X axis, (b) Y axis and (c) Z axis. For the hybrid distributed MIMO radar, the total number of elements is selected to be 100, the number of sub-arrays is set to be 4, each sub-array is with 5 × 5 elements, and these sub-arrays with are randomly distributed in a disk with a radius 5000m. The target is assumed to be located at $[0\text{m},0\text{m},10000\text{m}]^T$ with velocity $[10\text{m/s},10\text{m/s},100\text{m/s}]^T$.

assumed to be randomly located, the AFs shown in Fig.6 are the Monte Carlo result (100 times). Similarly, the distributed MIMO radar AFs are also the Monte Carlo results. It can be seen from this figure that the hybrid distributed MIMO radar can achieve much better position resolution than the PA radar, and the advantage mainly appears along the X-axis and Y-axis. Moreover, it can also be found that the hybrid MIMO radar provides a close position resolution as compared with the distributed MIMO radar. The main advantage of the hybrid distributed MIMO radar over the distributed MIMO radar is that much less orthogonal waveforms are needed. This will remarkably enhance the possibility of the engineering realization.

Secondly, we consider a moving target case, where the location is still fixed to be $[0\text{m},0\text{m},10000\text{m}]^T$ for both the ideal and real targets. The velocity parameter of the ideal target is set to be $[10\text{m/s},10\text{m/s},100\text{m/s}]^T$, and the velocity parameter of the real target is chosen to be varying in the vicinity of this value. The numerical results are shown in Fig.7. It can be seen from this figure that, the hybrid distributed MIMO radar can be able to provide a close 3-dimensional velocity resolution as compared with the distributed MIMO radar, while the PA radar can only resolve the radial velocity.

It is worth noting that to reduce the grating lobe phenomenon, the sub-arrays are randomly located in the simulations of Fig.6 and Fig.7. However, the derived ambiguity function of the hybrid distributed MIMO radar takes into account not only the effect of waveforms, but also that of the system geometry configuration. Therefore, if an optimized objective (cost function) is properly selected, there should be optimal positions to locate the sub-arrays. The detailed discussion of this issue is beyond the scope of this paper. This will be the research point in the next step.

Overall, as compared with the PA radar, the hybrid distributed MIMO radar can provide much better resolution both on position and velocity. While, as compared with the distributed MIMO radar, the hybrid MIMO radar can provide a close resolution using much less orthogonal waveforms.

VI. CONCLUSION

In this paper, a novel radar concept named hybrid distributed MIMO radar is proposed. The proposed hybrid distributed MIMO radar brings together the distributed MIMO radar concept and the phased array radar one, and thus it might be able to provide wide surveillance coverage, long dwell time, spatial diversity gains, and high resolution. As the first stage of studying the target detection and localization problems for hybrid distributed MIMO radar, this paper focuses on the issues of optimal detection and ambiguity function. Taking into account of the specific system configuration, the signal model of the hybrid distributed MIMO radar is re-derived using spatial Swerling-I target model. Then the optimal detector in the Neyman-Pearson sense is developed and the detection performance is evaluated. Furthermore, the AF of the hybrid distributed MIMO radar is developed. It is shown that the hybrid distributed MIMO radar AF is a general expression for the traditional MIMO radar and the PA radar. At last, some relevant numerical examples are presented. It is demonstrated that the hybrid distributed MIMO radar is capable to provide better detection performance of fluctuating targets than the PA and MIMO radars in many cases. Moreover, it is also shown that the hybrid distributed MIMO radar can provide

much better resolution both on position and velocity than the PA radar, and provide a close resolution, as compared with the distributed MIMO radar, using much less orthogonal waveforms. Theoretical results and numerical examples show that the proposed hybrid distributed MIMO radar is a promising technique. The next step of this research is to conduct the localization algorithm development and corresponding signal-level simulations.

APPENDIX

A. DERIVATION OF EQ.(21)

In this sub-section, we present the derivation of the likelihood functions of $\mathbf{r}(t)$ under the alternative hypothesis for the hybrid distributed MIMO radar, given in (42), as shown at the bottom of this page, where $\mathbf{b}_q^H \mathbf{w}_q = Q$ was assumed in the derivation, and c' is a negligible constant.

It should be pointed out that the integration term in the last line of (42) is a constant. Therefore, we can get

$$f\left(\mathbf{r}(t)|\mathcal{H}_1\right) = c_3 \cdot \exp\left[\frac{-\int \|\mathbf{r}(t)\|^2 \mathrm{d}t}{\sigma_n^2} + \frac{\frac{EQ^2}{M}\|\mathbf{X}\|^2}{\sigma_n^2\left(\sigma_n^2 + \frac{EQ^3}{M}\right)}\right] \tag{43}$$

where c_3 is a normalized constant that are ignored in the following derivations, $\mathbf{x} = [x_{11}, \ldots, x_{1K}, x_{21}, \ldots, x_{KK}]$ is the output of a bank of matched filters and

$$x_{pq} = \int \mathbf{a}_p^H \mathbf{r}_p(t) d_{pq}^*(t) s_q^*(t - \tau_{pq}) \mathrm{d}t \tag{44}$$

B. DERIVATION OF EQ.(33)

In this sub-section, we present the derivation of the relative entropy of the hybrid distributed MIMO radar, given in (45), as shown at the bottom of this page, where $\rho = E/\sigma_n^2$ is the SNR of the hybrid MIMO radar.

C. RELATIONSHIPS WITH OTHER RADAR SYSTEMS

If the number of sub-array K is decreased to 1, and $Q = M$, then the hybrid distributed MIMO radar will degrade into the traditional PA radar. In this case, the distribution of statistics, ROC, and the relative entropy of the hybrid MIMO radar can be rewritten as

$$T = \|\mathbf{X}\|^2 \sim \begin{cases} \left(\frac{Q^3 E}{2} + \frac{M\sigma_n^2}{2}\right) \cdot \chi_2^2, & \mathcal{H}_1\,; \\ \frac{M\sigma_n^2}{2} \cdot \chi_2^2, & \mathcal{H}_0\,; \end{cases} \tag{46}$$

$$\mathrm{P}_D = 1 - F_{\chi_2^2}\left(\frac{1}{M^2\rho + 1} \cdot F_{\chi_2^2}^{-1}(1 - \mathrm{P}_{FA})\right) \tag{47}$$

$$\mathrm{D}_{HM} = \ln\left(1 + \rho M^2\right) - \frac{\rho M^2}{1 + M^2} \tag{48}$$

If the number of sub-array K is increased to M, and $Q = 1$, then the hybrid distributed MIMO radar will degrade into the traditional distributed MIMO radar. In this case, the distribution of statistics, ROC, and the relative entropy of the hybrid

$$\begin{aligned} f\left(\mathbf{r}(t)|\mathcal{H}_1\right) &= \int f\left(\mathbf{r}(t)|\mathcal{H}_1, \boldsymbol{\alpha}\right) p(\boldsymbol{\alpha}) d\boldsymbol{\alpha} \\ &= \int c' \cdot \exp\left[-\frac{1}{\sigma_n^2}\int \sum_{p=1}^{K} \|\mathbf{r}_p(t) - \sqrt{\frac{E}{M}} Q \sum_{q=1}^{K} \alpha_{pq} \mathbf{a}_p d_{pq} s_q(t - \tau_{pq})\|^2 \mathrm{d}t\right] \cdot \exp\left[-\|\boldsymbol{\alpha}\|^2\right] d\boldsymbol{\alpha} \\ &= c' \exp\left[-\frac{\int \|\mathbf{r}(t)\|^2 \mathrm{d}t}{\sigma_n^2}\right] \cdot \int \exp\left[-\frac{1}{\sigma_n^2}\left(-\sqrt{\frac{E}{M}} Q \mathbf{X}^H \boldsymbol{\alpha} - \sqrt{\frac{E}{M}} Q \boldsymbol{\alpha}^H \mathbf{X} + \frac{EQ^3}{M}\|\boldsymbol{\alpha}\|^2\right)\right] \cdot \exp\left[-\|\boldsymbol{\alpha}\|^2\right] d\boldsymbol{\alpha} \\ &= c' \exp\left[-\frac{\int \|\mathbf{r}(t)\|^2 \mathrm{d}t}{\sigma_n^2} + \frac{\frac{EQ^2}{M}\|\mathbf{X}\|^2}{\sigma_n^2\left(\sigma_n^2 + \frac{EQ^3}{M}\right)}\right] \cdot \int \exp\left[-\frac{1}{\sigma_n^2}\left\|\sqrt{\sigma_n^2 + \frac{EQ^3}{M}}\boldsymbol{\alpha} - \frac{\sqrt{\frac{E}{M}} Q}{\sqrt{\sigma_n^2 + \frac{EQ^3}{M}}}\mathbf{X}\right\|^2\right] d\boldsymbol{\alpha} \end{aligned} \tag{42}$$

$$\begin{aligned} \mathrm{D}_{HM} &= \int \Gamma(K^2, Q\sigma_n^2) \cdot \ln\left(\frac{\Gamma(K^2, Q\sigma_n^2)}{\Gamma(K^2, Q^2\sigma_n^2 + Q^4 E/M)}\right) \mathrm{d}x \\ &= \int \Gamma(K^2, Q\sigma_n^2) \cdot \ln\left(\frac{\left(Q\sigma_n^2\right)^{-K^2} \cdot \exp\left[-\left(Q\sigma_n^2\right)^{-x}\right]}{\left(Q\sigma_n^2 + Q^4 E/M\right)^{-K^2} \cdot \exp\left[-\left(Q\sigma_n^2 + Q^4 E/M\right)^{-x}\right]}\right) \mathrm{d}x \\ &= K^2 \ln\left(\frac{Q\sigma_n^2 + Q^4 E/M}{Q\sigma_n^2}\right) \cdot \int \Gamma(K^2, Q\sigma_n^2) \mathrm{d}x + \left(\frac{1}{Q\sigma_n^2 + Q^4 E/M} - \frac{1}{Q\sigma_n^2}\right) \cdot \int x\Gamma(K^2, Q\sigma_n^2) \mathrm{d}x \\ &= K^2 \ln\left(\frac{Q\sigma_n^2 + Q^4 E/M}{Q\sigma_n^2}\right) + \left(\frac{1}{Q\sigma_n^2 + Q^4 E/M} - \frac{1}{Q\sigma_n^2}\right) \cdot K^2 Q\sigma_n^2 \\ &= K^2 \cdot \left(\ln\left(1 + \frac{\rho Q^3}{M}\right) - \frac{\rho Q^3}{M + \rho Q^3}\right) \end{aligned} \tag{45}$$

MIMO radar can be rewritten as

$$T = \|\mathbf{X}\|^2 \sim \begin{cases} \left(\frac{E}{2M} + \frac{\sigma_n^2}{2}\right) \cdot \chi^2_{2M^2}, & \mathcal{H}_1; \\ \frac{\sigma_n^2}{2} \cdot \chi^2_{2M^2}, & \mathcal{H}_0; \end{cases} \tag{49}$$

$$\mathrm{P}_D = 1 - F_{\chi^2_{2M^2}}\left(\frac{1}{\rho/M+1} \cdot F^{-1}_{\chi^2_{2M^2}}(1-\mathrm{P}_{FA})\right) \tag{50}$$

$$\mathrm{D}_{HM} = M^2 \cdot \left(\ln(1+\rho/M) - \frac{\rho}{M+\rho}\right) \tag{51}$$

It should be noted that the above expressions are coincident with corresponding results presented in [26], [27]. This indirectly proves the correctness of the results derived in this paper.

REFERENCES

[1] E. Fisher, A. Haimovich, R. Blum, D. Chizhik, L. Cimini, and R. Valenzuel, "MIMO radar, An idea whose time has come," in *Proc. IEEE Radar Conf.*, Honolulu, HI, USA, Apr. 2004, pp. 71–78.
[2] J. Li and P. Stoica, "MIMO radar with colocated antennas," *IEEE Signal Process. Mag.*, vol. 24, no. 5, pp. 106–114, Sep. 2007.
[3] A. M. Haimovich, R. S. Blum, and L. J. Cimini, "MIMO radar with widely separated antennas," *IEEE Signal Process. Mag.*, vol. 25, no. 1, pp. 116–129, Jan. 2008.
[4] Y. Li, S. A. Vorobyov, and V. Koivunen, "Ambiguity function of the transmit beamspace-based MIMO radar," *IEEE Trans. Signal Process.*, vol. 63, no. 17, pp. 4445–4457, Sep. 2015.
[5] H. Deng, B. Himed, and Z. Geng, "Mimo radar waveform design for transmit beamforming and orthogonality," *IEEE Trans. Aerosp. Electron. Syst.*, vol. 52, no. 3, pp. 1421–1433, Jun. 2016.
[6] H. Deng, "Polyphase code design for orthogonal netted radar systems," *IEEE Trans. Signal Process.*, vol. 52, no. 11, pp. 3135–3216, Nov. 2004.
[7] R. Kadlimatti and A. T. Fam, "Good code sets from complementary pairs via symmetrical/ antisymmetrical chips," *IEEE Trans. Aerosp. Electron. Syst.*, vol. 52, no. 3, pp. 1327–1339, Jun. 2016.
[8] N. H. Lehmann, A. M. Haimovich, R. S. Blum, and L. Cimini, "High resolution capabilities of MIMO radar," in *Proc. 40th Asilomar Conf. Signals, Syst. Comput.*, Sacramento, CA, USA, Nov. 2006, pp. 25–30.
[9] N. H. Lehmann, E. Fishler, A. M. Haimovich, R. S. Blum, D. Chizhik, L. J. Cimini, and R. A. Valenzuela, "Evaluation of transmit diversity in MIMO-radar direction finding," *IEEE Trans. Signal Process.*, vol. 55, no. 5, pp. 2215–2225, May 2007.
[10] Q. He, R. S. Blum, and A. M. Haimovich, "Noncoherent MIMO radar for location and velocity estimation: More antennas means better performance," *IEEE Trans. Signal Process.*, vol. 58, no. 7, pp. 3661–3680, Jul. 2010.
[11] Q. He, N. H. Lehmann, R. S. Blum, and A. M. Haimovich, "MIMO radar moving target detection in homogeneous clutter," *IEEE Trans. Aerosp. Electron. Syst.*, vol. 46, no. 3, pp. 1290–1301, Jul. 2010.
[12] R. Mudumbai, D. R. Brown, III, U. Madhow, and H. V. Poor, "Distributed transmit beamforming: Challenges and recent progress," *IEEE Commun. Mag.*, vol. 47, no. 2, pp. 102–110, Feb. 2010.
[13] A. J. Fenn, D. H. Temme, W. P. Delaney, and W. E. Courtney, "The development of phased-array radar technology," *Lincoln Lab. J.*, vol. 412, no. 2, pp. 321–340, Feb. 2000.
[14] B. Friedlander, "On the relationship between MIMO and SIMO radars," *IEEE Trans. Signal Process.*, vol. 57, no. 1, pp. 394–398, Jan. 2009.
[15] F. Daum and J. Huang, "MIMO radar: Snake oil or good idea?" in *Proc. 4th Int. Conf. Waveform Diversity Des. (WDD)*, Orlando, FL, USA, Feb. 2009, pp. 113–117.
[16] D. Fuhrmann and G. S. Antonio, "Transmit beamforming for MIMO radar systems using signal cross-correlation," *IEEE Trans. Aerosp. Electron. Syst.*, vol. 44, no. 1, pp. 171–186, Jan. 2008.
[17] J. P. Browning, D. R. Fuhrmann, and M. Rangaswamy, "A hybrid MIMO phased-array concept for arbitrary spatial beampattern synthesis," in *Proc. 13th IEEE Digit. Signal Process. Educ. Workshop*, Marco Island, FL, USA, Jan. 2009, pp. 446–450.
[18] D. R. Fuhrmann, J. P. Browning, and M. Rangaswamy, "Signaling strategies for the hybrid MIMO phased-array radar," *IEEE J. Sel. Topics Signal Process.*, vol. 4, no. 1, pp. 66–78, Feb. 2010.
[19] M. La Manna and D. R. Fuhrmann, "Target location estimation performance evaluation for a 2D hybrid-MIMO radar," in *Proc. IEEE Radar Conf.*, Seattle, WA, USA, May 2017, pp. 1603–1607.
[20] A. Hassanien and S. A. Vorobyov, "Phased-MIMO radar: A tradeoff between phased-array and MIMO radars," *IEEE Trans. Signal Process.*, vol. 58, no. 6, pp. 3137–3151, Jun. 2010.
[21] A. Hassanien and S. A. Vorobyov, "Transmit energy focusing for DOA estimation in MIMO radar with colocated antennas," *IEEE Trans. Signal Process.*, vol. 59, no. 6, pp. 2669–2682, Jun. 2011.
[22] F. A. Butt, I. H. Naqvi, and U. Riaz, "Hybrid phased-MIMO radar: A novel approach with optimal performance under electronic countermeasures," *IEEE Commun. Lett.*, vol. 22, no. 6, pp. 1184–1187, Jun. 2018.
[23] L. Xu and J. Li, "Iterative generalized-likelihood ratio test for MIMO radar," *IEEE Trans. Signal Process.*, vol. 55, no. 6, pp. 2375–2385, Jun. 2007.
[24] D. R. Fuhrmann, "MIMO radar signal processing for distributed phased arrays," in *Proc. 4th IEEE Int. Workshop Comput. Adv. Multi-Sensor Adapt. Process. (CAMSAP)*, Jun. 2011, pp. 1–4.
[25] I. Bekkerman and J. Tabrikian, "Target detection and localization using MIMO radars and sonars," *IEEE Trans. Signal Process.*, vol. 54, no. 10, pp. 3873–3883, Oct. 2006.
[26] E. Fishler, A. Haimovich, R. S. Blum, L. J. Cimini, D. Chizhik, and R. A. Valenzuela, "Spatial diversity in radars-models and detection performance," *IEEE Trans. Signal Process.*, vol. 54, no. 3, pp. 823–838, Mar. 2006.
[27] J. Tang, Y. Wu, Y. Peng, and X. Wang, "On detection performance and system configuration of MIMO radar," *Sci. China F, Inf. Sci.*, vol. 52, no. 7, pp. 1250–1257, Jul. 2009.
[28] J. Xu, X.-Z. Dai, X.-G. Xia, L.-B. Wang, J. Yu, and Y.-N. Peng, "Optimizations of multisite radar system with MIMO radars for target detection," *IEEE Trans. Aerosp. Electron. Syst.*, vol. 47, no. 4, pp. 2329–2343, Oct. 2011.
[29] M. T. Frankford, K. B. Stewar, N. Majurec, and J. T. Johnson, "Numerical and experimental studies of target detection with MIMO radar," *IEEE Trans. Aerosp. Electron. Syst.*, vol. 50, no. 2, pp. 1569–1577, Apr. 2014.
[30] P. M. Woodward, *Probability and Information Theory With Application to Radar*. Oxford, U.K: Pergamon, 1953.
[31] G. S. Antonio, D. R. Fuhrmann, and F. C. Robey, "MIMO radar ambiguity functions," *IEEE J. Sel. Topics Signal Process.*, vol. 1, no. 1, pp. 167–177, Jun. 2007.
[32] T. Derham, S. Doughty, C. Baker, and K. Woodbridge, "Ambiguity functions for spatially coherent and incoherent multistatic radar," *IEEE Trans. Aerosp. Electron. Syst.*, vol. 46, no. 1, pp. 230–245, Jan. 2010.
[33] H. Chen, Y. Chen, Z. Yang, and X. Li, "Extended ambiguity function for bistatic MIMO radar," *J. Syst. Eng. Electronics.*, vol. 23, no. 2, pp. 195–200, Apr. 2012.
[34] M. Radmard, M. M. Chitgarha, M. N. Majd, and M. M. Nayebi, "Ambiguity function of MIMO radar with widely separated antennas," in *Proc. 15th Int. Radar Symp. (IRS).*, Jun. 2014, pp. 1–5.
[35] A. Guruswamy and R. Blum, "On a definition of the ambiguity function for non-coherent radars," in *Proc. IEEE 7th Workshop Sensor Array Multichannel Signal Process.*, Jun. 2012, pp. 141–144.
[36] C. V. Ilioudis, C. Clemente, I. Proudler, and J. Soraghan, "Ambiguity function for distributed MIMO radar systems," in *Proc. IEEE Radar Conf.*, Philadelphia, PA, USA, May 2016, pp. 1–6.
[37] C. Y. Chen and P. P. Vaidyanathan, "MIMO radar ambiguity properties and optimization using frequency-hopping waveforms," *IEEE Trans. Signal Process.*, vol. 56, no. 12, pp. 5926–5936, Dec. 2008.
[38] Y. I. Abramovich and G. J. Frazer, "Bounds on the volume and height distributions for the MIMO radar ambiguity function," *IEEE Signal Process. Lett.*, vol. 15, pp. 505–508, May 2008.
[39] A. Guruswamy and R. Blum, "Ambiguity optimization for frequency-hopping waveforms in MIMO radars with arbitrary antenna separations," *IEEE Signal Process. Lett.*, vol. 23, no. 9, pp. 1231–1235, Sep. 2016.
[40] M. Skolnik, *Introduction to Radar Systems*, 3rd ed. New York, NY, USA: McGraw-Hill, 2002.
[41] M. Abramowitz and I. A. Stegun, *Handbook of Mathematical Functions with Formulas, Graphs, and Mathematical Tables*, 9th ed. New York, NY, USA: Dover, 1972.

[42] L. L. Scharf, *Statistical Signal Processing: Detection, Estimation, and Time Series Analysis*, London, U.K.: Pearson, 2002.
[43] T. M. Cover and J. A. Thomas, *Elements of Information Theory*, New York, NY, USA: Wiley, 1991.

QILEI ZHANG was born in Gansu, China. He received the B.S. degree in communication engineering, and the M.S. and Ph.D. degrees in information and communication engineering from the National University of Defense Technology (NUDT), Changsha, in 2007, 2009, and 2014, respectively.

From January 2012 to July 2013, he was a Visiting Ph.D. Student with the University of Birmingham, Birmingham, U.K. He is currently an Associate Professor with the National University of Defense Technology. His fields of interests include signal processing, synthetic aperture radar, and ionosphere.

ZHEN DONG was born in Anhui, China, in September 1973. He received the Ph.D. degree in electrical engineering from the National University of Defense Technology (NUDT), Changsha, in 2001.

He is currently a Professor with the College of Electronic Science and Technology, NUDT. His recent research interests include SAR system design and processing, ground moving target indication (GMTI), and digital beamforming (DBF).

DEXIN LI was born in Henan, China, in January 1989. He received the B.S. degree in electronic information engineering from Xidian University, Xi'an, China, in 2007, and the M.S. and Ph.D. degrees in information and communication engineering from the National University of Defense Technology (NUDT), Changsha, China, in 2013 and 2017, respectively.

From 2015 to 2017, he was a joint-Ph.D. Student with the Microwaves and Radar Institute, German Aerospace Center (DLR), Oberpfaffenhofen, Germany. He is currently a Lecturer with the College of Electronic Science, NUDT. His research interests include SAR image formation and signal processing.